DEVELOPMENT OF NOVEL BIOMEDICAL MATERIALS FOR 3DP MACHINE BASED ON NATURAL POLYMERS

PASSAKORN TESAVIBUL

A THESIS SUBMITTED IN PARTIAL FULFILLMENT
OF THE REQUIREMENTS FOR
THE DEGREE OF MASTER OF ENGINEERING
(BIOMEDICAL ENGINEERING)
FACULTY OF GRADUATE STUDIES
MAHIDOL UNIVERSITY
2004

ISBN 974-04-5361-9

Thesis
Entitled

DEVELOPMENT OF NOVEL BIOMEDICAL MATERIALS FOR 3DP MACHINE BASED ON NATURAL POLYMERS

Passakorn Tesavibul
.....
Mr. Passakorn Tesavibul
Candidate

Jintamai Suwanprateeb
.....
Mr. Jintamai Suwanprateeb, Ph.D.
Major-Advisor

Theeraporn Rubcumintara
.....
Asst.Prof.Theeraporn Rubcumintara
Ph.D.
Co-Advisor

Rassm Hoon
.....
Assoc.Prof.Rassmidara Hoonsawat
Ph.D.
Dean
Faculty of Graduate Studies

Theeraporn Rubcumintara
.....
Asst.Prof.Theeraporn Rubcumintara
Ph.D.
Chair
Master of Engineering
Programme in Biomedical Engineering
Faculty of Engineering

Thesis
Entitled

DEVELOPMENT OF NOVEL BIOMEDICAL MATERIALS FOR 3DP MACHINE BASED ON NATURAL POLYMERS

was submitted to the Faculty of Graduate Studies, Mahidol University
for the degree of Master of Engineering (Biomedical Engineering)

on
Oct 15, 2004

Passakorn Tesavibul
.....
Mr. Passakorn Tesavibul
Candidate

Jintamai Suwanprateeb
.....
Mr. Jintamai Suwanprateeb, Ph.D.
Chair

Theeraporn Rubcumintara
.....
Asst.Prof.Theeraporn Rubcumintara
Ph.D.
Member

Udom Tipayamontri
.....
Asst.Prof.Udom Tipayamontri
Ph.D.
Member

Khemchai Hemachandra
.....
Assoc.Prof.Khemchai Hemachandra
Ph.D.
Member

Rassmidara Hoonsawat
.....
Assoc.Prof.Rassmidara Hoonsawat,
Ph.D.
Dean
Faculty of Graduate Studies
Mahidol University

Piya Rattanasuwan
.....
Asst.Prof.Piya Rattanasuwan
Dean
Faculty of Engineering
Mahidol University

ACKNOWLEDGEMENTS

I would like to thank my major advisor, Dr.Jintamai Suwanprateeb who helped me in all the time of research and writing of this thesis. I am also grateful to Dr.Theeraporn Rubcumintara, my co-advisor, whose stimulating and suggestion.

I am deeply indebted to National Metal and Materials Technology Center (MTEC) for research resources and location.

Especially, I would like to give my special thanks to my mother for fully support and encouragement throughout this thesis.

Passakorn Tesavibul

DEVELOPMENT OF NOVEL BIOMEDICAL MATERIALS FOR 3DP MACHINE BASED ON NATURAL POLYMERS.

PASSAKORN TESAVIBUL 4436901 EGBE/M

M.Eng.(BIOMEDICAL ENGINEERING)

THESIS ADVISORS: JINTAMAI SUWANPRATEEB, Ph.D., THEERAPORN RUBCUMINTARA, Ph.D.

ABSTRACT

Three Dimensional Printing or 3DP, a rapid prototyping technique that produces 3D physical models from computational 3D images, is used to fabricate an implant model from individual medical images from a patient. However, general rapid prototyping materials cannot be implanted directly into the body. Thus, a Rapid Prototyping model is normally used to generate a set of moulds to cast the implant, usually made from bone cement or polymethyl methacrylate (PMMA), leading to the extra cost of silicone mould material and the risk of model damage from unnecessary material handling and mould imperfection.

This thesis reported the development of suitable material based on a blend of various natural polymers that are biocompatible for processing in a 3DP machine and compared the properties of these materials with the original 3DP material. It was observed that the most suitable formulation consisted 40% starch, 40% dextrin and 20% gelatin. When compared to the original 3DP material which is a plaster based material, the experimental material has higher shrinkage but lower density and mechanical properties than the original sample, for both drying and non-drying samples.

KEY WORDS: RAPID PROTOTYPING / THREE DIMENSIONAL PRINTING / NATURAL POLYMER / BIOMEDICAL MATERIALS / MECHANICAL PROPERTIES

50 P. ISBN 974-04-5361-9

การพัฒนาวัสดุทางการแพทย์ชนิดใหม่ สำหรับเครื่องพิมพ์สามมิติ จากพอลิเมอร์ธรรมชาติ
(DEVELOPMENT OF NOVEL BIOMEDICAL MATERIALS FOR 3DP MACHINE BASED ON NATURAL POLYMERS)

ภาสกร เทศะวิบุล 4436901 EGBE/M

วศ.ม. (วิศวกรรมชีวการแพทย์)

คณะกรรมการควบคุมวิทยานิพนธ์ : จินตมัย สุวรรณประทีป, Ph.D., ธีรพร รับคำอินทร์, Ph.D.

บทคัดย่อ

เครื่องพิมพ์สามมิติเป็นเครื่องสร้างต้นแบบรวดเร็วที่สามารถสร้างแบบจำลองสามมิติจากภาพสามมิติในคอมพิวเตอร์ ซึ่งได้ถูกใช้ในการสร้างแบบจำลองวัสดุฝังในโดยใช้ภาพถ่ายทางการแพทย์ของผู้ป่วยโดยตรง อย่างไรก็ตาม วัสดุที่ใช้ทำแบบจำลองโดยทั่วไปไม่สามารถนำไปใช้ในร่างกายได้โดยตรง จึงต้องนำไปสร้างแม่พิมพ์เพื่อใช้ในการหล่อวัสดุฝังในซึ่งทำจากซีเมนต์กระดูกหรือพอลิเมทิล เมทาคริเลต ทำให้ต้องเสียค่าใช้จ่ายเพิ่มขึ้นจากการทำแม่พิมพ์ และเกิดความเสี่ยงที่แบบจำลองจะเสียหายจากการเคลื่อนย้ายหรือความไม่สมบูรณ์ของแม่พิมพ์

วิทยานิพนธ์ฉบับนี้ กล่าวถึงการพัฒนาส่วนผสมจากพอลิเมอร์ธรรมชาติ ที่มีความเข้ากันได้ทางชีวภาพ เพื่อให้เหมาะสมที่จะใช้กับเครื่องพิมพ์สามมิติ ซึ่งพบว่าสัดส่วนที่เหมาะสมจะประกอบไปด้วย แป้ง ร้อยละ40 เด็กซ์ทริน ร้อยละ40 และเจลาติน ร้อยละ20 เมื่อนำมาเปรียบเทียบกับวัสดุเดิมที่เป็นวัสดุประเภท พลาสเตอร์แล้ว พบว่าวัสดุใหม่มีการหดตัวมากกว่า แต่มีความหนาแน่น และสมบัติทางกลน้อยกว่าวัสดุเดิม ทั้งในแบบที่ผ่านการอบแล้ว และยังไม่ได้อบ

50 หน้า. ISBN 974-04-5361-9

CONTENTS

CONTENTS (Cont.)

LIST OF TABLES

LIST OF FIGURES

LIST OF FIGURES (Cont.)

CHAPTER I
INTRODUCTION

Background

Rapid Prototyping (RP) Technology is a manufacturing process that fabricates three-dimensional model by using solid freeform fabrication (SFF) techniques. The system uses 3D computer data to form the physical objects by adding and bonding materials layer by layer with a high degree of accuracy. Consequently, this technology can form object, which have complicated shape and details, faster than the traditional model building techniques [1,2].

Three Dimensional Printing or 3DP is the one of several kinds of RP. This technique is interested because of its simple process and ability to use a wide range of materials including metals, ceramics and polymers. The system begins with the multi-channel jetting head deposits a liquid binder onto the top layer of a bed of powder material. The particles of the powder are bonded in the areas where the binder is deposited. When a layer is completed, the piston will move down by the thickness of a layer. The piston of the powder supply bed moves upward incrementally to supply powder for the process and the roller spreads and compresses the powder on the top of the build section. The process is repeated until the entire object is completed within the powder bed [2,3].

Recently, rapid prototyping technologies have been used in medical field because of the ability to process medical image data and to facilitate computer model manipulation. For orthopedic implantation, an individual patient's particular morphology image, which is recorded using Magnetic Resonance Imaging (MRI) or Computed Tomography (CT) scanning devices, is converted into a three-dimensional model in STL file. The implant model is designed by mirroring symmetrical profile onto the defect. This model, which perfectly fits the defect, is fabricated by RP [4].

However, general rapid prototyping materials are designed for industrial works, so the parts cannot be implanted directly into the body. Thus, RP model is normally used to generate a set of mould to cast the implant that is usually made from bone cement or PMMA (Polymethylmethacrylate).

Objective

The objective of this thesis is to formulate the blend of natural polymers that are biocompatible and able to be fabricated by 3DP, and to compare the properties of these materials with the original 3DP material.

Scope

The 3DP model fabricated from the experimental material, which is the blend of natural organic substances such as starch, cellulose fiber, dextrin, pregelatinized starch and gelatin, will be formulated and characterized in terms of physical and mechanical properties such as density, porosity, shrinkage, bending and compression strength to compare to the model fabricated from original 3DP material.

Expected Results

Biomaterial can be fabricated directly from 3DP, the step of generating a set of silicone mould will be skipped. In addition, the extra costs of silicone mould material will be saved. Beside, this technique not only makes the process more convenient, but it also reduces the risk of model damages from unnecessary material handling and mould imperfection.

CHAPTER II
LITERATURE REVIEW

1. Rapid Prototyping Technology

1.1 Overview

Rapid Prototyping (RP) is a technique that fabricates a physical three-dimensional object directly from graphical data for example computer aided design (CAD) files. The object is printed sequentially layer by layer until the entire 3D structure is built.

There are several types of RP, available in the market with the difference in process and the using materials, such as Stereolithography (SLA), Selective Laser Sintering (SLS), Fused Deposition Modeling (FDM), Laminated Object Manufacturing (LOM) and Three Dimensional Printing (3D Printing) [3].

1.2 Stereolithography (SLA)

Stereolithography (SLA) forms an object by tracing a laser beam on the surface of a vat of liquid photopolymer, a resin that solidifies when exposed to light. Objects that have overhang or undercut must be supported automatically or with human interaction. The support will be removed when the work has been finished. Finally, the object needs to be cured with UV light in an oven for increasing material strength.

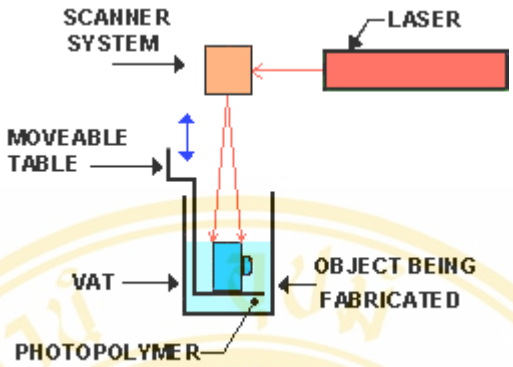

Figure 1 Stereolithography (SLA), [2]

1.3 Selective Laser Sintering (SLS)

Selective Laser Sintering (SLS) uses laser beam to melt and bond powdered material, which is heated just below the melting point. The layer is added from a power cartridge by the powder-leveling roller and the built platform moves down incrementally. Supports are not required for this system since overhangs and undercuts are supported by the powder bed.

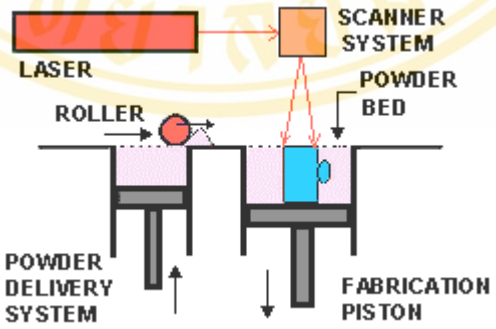

Figure 2 Selective Laser Sintering (SLS), [2]

1.4 Fused Deposition Modeling (FDM)

Fused Deposition Modeling (FDM) is the RP system that melts the material such as ABS, wax, nylon, polycarbonate, polyethylene and polypropylene. The material which is filament is heated in a nozzle, and the molten material is extruded to form an object. A second filament is used for building up the supports, which are easily removable using a force or water-based solution that dissolves them.

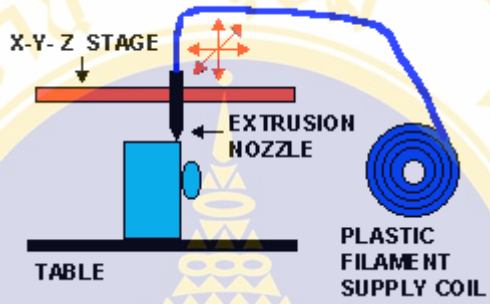

Figure 3 Fused Deposition Modeling (FDM), [2]

1.5 Laminated Object Manufacturing (LOM)

Laminated Object Manufacturing (LOM) was material sheets which are coated with an adhesive. The sheet is cut by a laser or blade, according to the required shape. The next layer is fed on top and connected by a heated roller that activates the adhesive. This process is self-supporting for overhangs and undercuts.

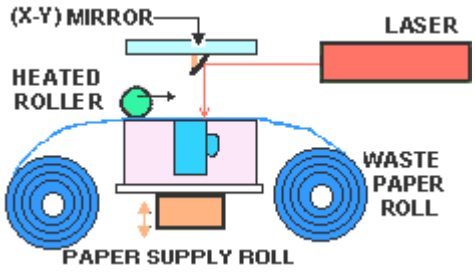

Figure 4 Laminated Object Manufacturing (LOM), [2]

1.6 Three Dimensional Printing (3DP)

Three Dimensional Printing (3DP) uses the inkjet print head to spray the liquid binder to bond the powder materials which is distributed and compressed by the roller. This technique needs no external support during fabrication since the powder bed supports overhangs and undercuts. After completion, the object is elevated and the excess powder is brushed away leaving a "green" object. Finally, the part may be infiltrated for greater strength. A variety of materials can be used, such as resin, wax or epoxy, depending on the objectives of the parts.

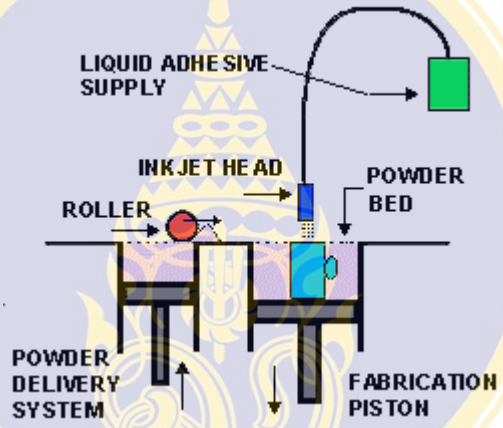

Figure 5 Three Dimensional Printing (3DP), [2]

2. Applications of Rapid Prototype

Because of the ability to create a complex geometry with relatively high accuracy, quick process and wide materials selection, the rapid prototyping technology is widely used in many fields [1].

- In engineering, the models are used for design studies and functional trial. Many parts for the space shuttle fleet, F-18 fighter jets and F1 racing cars are developed using this technology. The scientists also have the idea that to have a RP machine on board of the International Space Station (ISS) to produce spare parts for repair jobs.

- In architecture, rapid prototyping technology is used for teaching students about the new possibilities in testing their draft for lighting conditions and mechanical details.
- In art and archeology, the original ancient statues which suffer from environmental influences are scanned to derive the 3D data. Then the software is used to correct the damages and the duplicate parts are created by Selective Laser Sintering with marble powders.
- In science, RP is used to create the upscale molecular chains models for demonstration purpose in the classroom.
- In medical, medical imaging from CT or MRI is converted in to 3D image such as STL file. Then the medical model can be made individually with a high precision and resolution [1,4].

In case of medical application, the RP model from the individual patient helps surgeon in pre-operative planning discussion, explains complex operations especially craniofacial and maxillofacial surgeries and helps medical student to get more comprehensive in anatomy. In orthopedic surgery, this technique increases the quality of treatment because RP model was created from computational 3D image that can be optimized in term of geometric and surface morphology. Then an implantation using bone cement which is cast from the RP model not only reduced operating times and complication but also avoided the risk of tissue damage from heat that bone cement had generated in the conventional implantation [4].

The next major application is producing customized drilling guides. When a patient has suffered spinal trauma such that parts of the spinal column are damaged or has deformation of the spine through disease or birth defect, they may need for plates to be attached to individual vertebrae to prevent the movement. Similarly in dental surgery, when a patient requires dental implants, screws are attached into the upper or lower jaw onto which teeth replacements are attached. In both cases there is a need to drill into a limited quantity of bone tissue in the spine or jaw, which must be strong enough to support the implant. The production of drilling guide template for spinal or dental surgery serves the requirement of highly accurate drilling. These templates are then produced directly by a rapid prototyping technique and once a metal sleeve is inserted into the drilling guide and the whole template is sterilized, it is ready for use.

In bone tissue engineering field, the flexibility and outstanding manufacturing capability of RP have been employed for the application. RP technique can be used to generate porous ceramics as bone substitutes, which is called scaffolds. The scaffolds, built from synthetic or natural materials, serve as temporary surrogates for the native extra-cellular matrix (ECM). Scaffold-based tissue engineering is used to construct biologic replicas *in vitro* such that the engineered composite becomes integrated for transplantation *in vivo* for the recovery of loss or malfunctioned tissues or organ. In RP application, patient specific data and scaffold structural properties required for regenerating specific tissues can be incorporated into the scaffold design via CAD. The use of CAD will allow user control over localized pore morphologies and porosity to suit the requirements of different cell types within the same scaffold volume. In addition, some RP techniques allow pharmaceutical and biological agents to be incorporated into the scaffolds during fabrication [5].

3. The Use of Biomaterials in Rapid Prototyping Technology

Most of medical RP researches usually focuses on bone prosthesis or scaffolds fabrication for tissue engineering. Many papers show that the scaffold can be created from many kind of material by many RP techniques such as a blended of diethyl fumarate (DEF) and polypropylend fumarate (PPF) in SLA, calcium phosphate powder in SLS, polycaprolactone (PCL) in FDM and polylactide-coglycolide (PLGA) in 3DP.

3.1 LOM

Rapid prototyping technique such as LOM system can be used to construct a non-resorable bioceramic composite. A calcium hydroxyapatite particle, bonded by a calcium phosphate glass phase, was formed into thin ceramic sheets (125-250 μm) using a tape-casting process [6]. Then, this material was constructed by LOM system.

3.2 SLA

For SLA, the experiments used SLA was used to fabricate the biodegradable scaffolds for bone implantation, a biodegradable resin consisted of diethyl fumarate (DEF), poly (propylene fumarate) (PPF), and a photoinitiator, bisacylphosphine oxide (BAPO). The PPF was crosslinked with the use of the SLA equipped with a UV laser, 325-nm wavelength [7].

3.3 SLS

Calcium phosphate powders were prepared by reacting hydroxyapatite with phosphoric acid [8]. Then, the powders were coated with an intermediate polymer binder, poly (methyl methacrylate-(o-n-butyl methacrylate) (PMMA) emulsion copolymer, by sprayed drying different slurries containing 30 vol% polymer emulsion and ceramic powders. This powder was used to form an object by SLS. After binder burnout and sintering cycle, the mechanical strengths were reported to be about 18.6 MPa at densities of 1.4 g/cm^3. After infiltration with a diluted solution of phosphoric acid based inorganic cement, the parts exhibited an increased density to 1.25 g/cm^3 with strengths at 7.6 MPa. Pore sizes were reported about 50 μm. The others materials that have been investigated for SLS are polyetheretherketone (PEEK) and hydroxyapatite (HA) [9]. The feasibility of sintering such a blended mixtures of PEEK and HA and the influence of SLS process parameters on the sintering quality and resulting microstructure of sintered specimens were studied.

3.4 FDM

FDM technique was used for producing polycaprolactone (PCL) scaffolds with different geometrically consistent honeycomb-like patterns [10]. The scaffolds ware constructed with pore sizes ranging from 160 to 700 μm and 48% to 70% porosities. Different designs of porosities ware obtained by varying the laydown patterns, while the channel sizes were varied by the spacing between the extruded roads of polymeric material. Compressive stiffness of the scaffold was between 4 and 77 MPa and 0.4 to 3.6 MPa for yield strengths depending on the laydown pattern and other processing parameters. FDM technique was also developed for extruding ceramic materials, which is called FDC (fused deposition of ceramics). FDC used β-tricalcium phosphate

(TCP) as the feedstock for a ceramic composite [11]. Porous scaffolds were fabricated ranging from 0.20 to 1.26 mm for road and 0.30 to 1.90 mm for channel widths. The scaffold had 16% of shrinkage in the x-direction and 18% in both the y- and z-directions.

3.5 3DP

A wide range of biomaterials were investigated as a 3DP material, some of material properties that may effect to the fabrication have been concerned and studied for example, the simultaneous spreading, infiltration properties of liquid binder on powder material. The porous scaffolds were created by using polylactide-coglycolide (PLGA) powder mixed with salt particles and a suitable organic solvent [12]. After the process, the salt particles ware leached by distilled water to create 45-150 μm pore sizes with 60% porosity. The researchers also used 3DP to fabricate a porous of poly (L-lactic acid) (L-PLA) disc shaped scaffolds, 10 mm diameter and 2 mm height, to investigate the influence of pore size and porosity on cell adhesion.

In addition, the natural polymers, a blend of starch based powder, containing cornstarch (50%), dextran (30%) and gelatin (20%), was also used to fabricate the scaffold by 3DP [13]. The porosities of the scaffolds ware 51% for structure with in-built channels. After infiltrate with copolymer solution, containing 75% poly (L-lactide) acid and 25% poly capolactone in dichloromethane, the porosity ware decreased to 54.7% for the solid cylinders design and between 33.5% and 43.9% for the structures with in-built channels. Therefore, the results showed that the polymer infiltration improves the scaffold's mechanical strengths and water resistance. Although, this research has not presented the biocompatibility of the scaffold or each natural polymer, there are some papers to support this property.

4. Biocompatibility of Natural Polymers

Starch-based materials (starch/ethylenl vinyl alcohol blend, SEVA-C) and a composite of SEVA-C reinforced with hydroxyapatite (HA) particles were evaluated in both *in vitro* and *in vivo* biocompatibility tests [14]. For the *in vitro* analysis cell culture method were used, according to ISO/EN 10993 part 5 guidelines. In case of *in*

vivo tissue reactions were evaluated in an intramuscular and intracortical bone implantation model on goats, using light and scanning electron microscopy. A computerized image analysis system was also used to obtain histomorphomeric data regarding bone contact and remodeling after 6 and 12 weeks of implantation. In both in vitro and in vivo models, the starch-based materials did not show relevant toxicity. Another starch-based material that was assessed by cytotoxicity and cell adhesion tests was a blended of starch and cellulose acetate (SCA) [15]. The result showed that both types of starch-based polymers (SEVA-C and SCA) exhibited a cytocompatibility that might allow for their use as biomaterials. For gelatin, the IPN (interpenetrating polymer networks) based on gelatin and poly(1-vinyl-2-pyrrolidinone) were tested to investigate the *in vitro* biocompatibility and hemocompatibility [16]. The materials did not interfere on cellular functions and neither induced platelet adhesion. For the others natural polymers, pregelatinized starch and maltodextrin can be used in pharmaceutical tablets, and pregelatinized starch also has the potential of a constant release rate for an extended period of time in drug control release system [17-18]. Cellulose fiber is a food grade that is used as a fiber source [19].

CHAPTER III
RESEARCH METHODOLOGY

3.1 Materials and Equipment

The Rapid Prototyping machine used in this study is the 3D printer (Z400 system, Z Corporation, USA). Natural polymers including tapioca starch (Thai Wah Public, Thailand), maltodextrin (Shandong, China), gelatin (Geltech, Korea), pregelatinized starch (Thai Wah Public, Thailand) and cellulose fiber (Sunoppa, USA.) were used as raw materials.

Starch, consisting of repeating glucose units, is composed of polysaccharides amylose and amylopectin. Amylose consists of straight chains containing 200 to 2,100 glucose units while amylopectin consists of branched chains containing 20 to 25 glucose units each. Maltodextrin is a short chain saccharide polymers obtained from the partial acid or enzymatic hydrolysis of starch. It consists of D-glucose units linked principally by alpha-1, 4 bonds. It has a dextose equivalent of less than 20 and basically is not sweet and is not fermentable. It has fair solubility. It functions as a body agent, bulking agent, texturizer, carrier, and crystallization inhibitor. Gelatin is a protein that functions as a gelling agent. It is obtained from collagen derived from beef bones and calfskin or pork skin. Pregelatinzed starch is a starch that has been processed to permit swelling in cold water, unlike natural starch which requires heating. The processing usually consists of cooking starch slurries, drying, and grinding to a fine powder. Cellulose is a carbohydrate polymer made up of glucose units. It consists of fibrous particles and is used as a fiber source and bulking agent in low-calorie formulations [20].

3.2 Experimental Procedures

3.2.1 Preliminary Observation

Each natural polymer was spread by roller and water was dropped to observe the behaviors that are relevant to the printing process on 3DP such as spreading, absorption, surface roughness, drying time and strength after drying compare to the original powder material.

3.2.2 Samples Preparation

Various blends of natural polymers were formulated in order to adjust the properties to be closed to the 3DP material. A proper formula was printed on 3DP machine with water-based binder by varying the printing conditions such as layer thickness and saturation. Rectangular bars (1038034 mm) were prepared for dimensional measurement and flexural test. Square bars (1031034 mm) were used to investigate density and porosity while and cylinder pieces was printed to determine the compressive strength. The specimens were divided into four groups, S1-1, S1-2, P-1 and P-2 for non-drying and drying experimental samples, and for non-drying and drying original samples, respectively. For drying, the specimens were dried at 70°C for 15 minutes after printing.

3.2.3 Characterization

3.2.3.1 Particle Size Analysis

Particle sizes of the experimental powder materials were determined using a particle size analyzer (Mastersizer-S, Malvern Instruments, UK.) which uses a laser diffraction technique. According to the Fraun Hofer approximation and Mie theory, when the particles, which spread in the media, cross to the light, the intensity of the diffracted light will be proportional to the amount of the particles in each size. Thus, with the light detector and computer, the diffraction data can be used to estimate the particle size distribution. This test was performed with dry type using 300 mm range lens and 2.4 mm beam length which are the standard parameters for dry dispersions in air media.

3.2.3.2 Dimensional Measurement

All of the test bars were measured using a digital vernier with 0.01 mm resolution. The observed dimensions were compared with the setting dimension to determine the accuracy. Non-drying objects were compared with the drying objects to determine the shrinkage. Dimensional error and shrinkage were calculated by

$$X_e = X_m - X_s$$

$$S = (X_2 - X_1) / X_1$$

where X_e is a dimensional error (mm)

X_m is a measured dimension (mm)

X_s is a setting dimension (mm)

S is shrinkage

X_1 is a dimension before drying (mm)

X_2 is a dimension after drying (mm)

3.2.3.3 Apparent Density Determination

The test specimens were weighed on a digital scale (PB4002-S, Mettler Toledo, Switzerland) with 0.01 gram resolution. The apparent density was calculated by

$$D = W / V_a$$

where D is a density of specimen (Kg./m^3)

W is a weight of specimen (Kg.)

V_a is an apparent volume of specimen (m^3) while V_a is calculated from the measured dimension.

3.2.3.4 Porosity Analysis

Porosity of specimens was measured by a gas pycnometer (Ultrapycnometer 1000, Quanta Chrome, USA.). It uses an inert gas such as Helium, which can penetrate into small pores down to approximate 10 nm without capillary force problems, to measure the true volume of materials by Archimedis principle of fluid or gas displacement. Porosity was calculated by the general formula

$$P = (V_a - V_t) / V_a$$

where P is a porosity and V_t is a true volume (m^3)

3.2.3.5 Bending Test

Three point bending test is done in accordance with ASTM D790 using universal testing machine (Instron 4502, USA). The test bars were rested on two supports with 64 mm span and were loaded by means of a loading nose midway between the supports at the speed of 1.9 mm/min. The tests were performed at 23 ± 2°C and 50 ± 5% relative humidity.

3.2.3.6 Compressive Test

Test specimens were placed between the surfaces of the compression tool on universal testing machine (Instron 4502, USA). It was ensure that the ends of the specimen were parallel with the surface of the compression tool in accordance with ASTM D695. The test specimens were load at a speed of 1.3 mm/min and the maximum compressive loads were recorded to calculate the compressive strength by dividing it by the minimum cross-sectional area of the specimen. The tests were performed at 23 ± 2°C and 50 ± 5% relative humidity.

CHAPTER IV
RESULTS

Particle Sizes

Average particle sizes of materials are shown in Table 1. Starch particle is the smallest in diameter and the gelatin particle is the largest. Cellulose fiber is larger than both pregelatinized.

Table 1 Particle sizes of materials

Samples	Volume Distribution			Mean Diameters (μm)
	10%	50%	90%	
Starch	9.21$_6$ 0.09	19.82$_6$ 0.28	46.06$_6$ 1.98	25.37$_6$ 0.79
Dextrin	32.73$_6$ 0.14	83.08$_6$ 0.25	160.06$_6$ 0.42	90.35$_6$ 0.29
Gelatin	79.48$_6$ 1.43	226.24$_6$ 2.82	512.49$_6$ 2.38	264.94$_6$ 2.61
Pregelatinized Starch	30.55$_6$ 0.03	88.19$_6$ 0.21	178.35$_6$ 0.65	97.29$_6$ 0.32
Cellulose Fiber	17.80$_6$ 0.16	103.72$_6$ 0.38	258.30$_6$ 1.95	123.78$_6$ 1.03

Preliminary Observation

It was observed that the characteristics of the powder layer which was dropped by water droplet were different. Starch did not show shrinkage as much as dextrin but it was weak after drying (figure 6), while dextrin was not weak (figure 7). Gelatin (figure 8) and pregelatinized starch (figure 9) turned to gel immediately after water was dropped. Thus, both did not exhibit the over spreading and shrinkage but gelatin has a higher strength after drying than pregelatinized starch. Cellulose fiber did not gel but its surface was swell after drying (figure 10).

From the experimental blended formulas, the greater percentages of starch resulted in lower shrinkage and lower strength (figure 11), which was in contrast with dextrin (figure 12). Thus, the ratio of starch in the component should equal to dextrin (figure 13). Gelatin, pregelatinized starch and cellulose fiber characteristics could prevent the over spreading but gelatin had higher strength than pregelatinized starch (figure 14) and did not swell as cellulose fiber (figure 15). Based on results in Table 2, the proper formula in this preliminary study consisted of 40 wt. % starch, 40 wt. % dextrin and 20 wt. % gelatin (figure 16).

Besides, the strengths were defined by the characteristics after dipped with needle. If the needle was not able to dip through the sample it was defined to good. The sample was defined to poor if the sample can dip through the sample and the sample was broken but if the sample was not broken it was defined to moderate.

Table 2 Characteristics of samples when they were dropped by water droplet

Samples	Characteristics			
	shrinkage	over spreading	strength	swelling
starch	none	high	poor	none
dextrin	high	none	good	none
gelatin	none	low	moderate	none
pregelatinized starch	none	low	poor	none
cellulose fiber	none	low	moderate	high
80%starch 20%dextrin	low	high	poor	none
20%starch 80%dextrin	high	low	good	none
50%starch 50%dextrin	moderate	moderate	moderate	none
40%starch 40%dextrin 20%gelatin	low	low	moderate	none
40%starch 40%dextrin 20%pregelatinized starch	low	low	poor	none
40%starch 40%dextrin 20%cellulose fiber	none	low	moderate	low

Figure 6 Starch which was dropped by water droplet

Figure 7 Dextrin which was dropped by water droplet

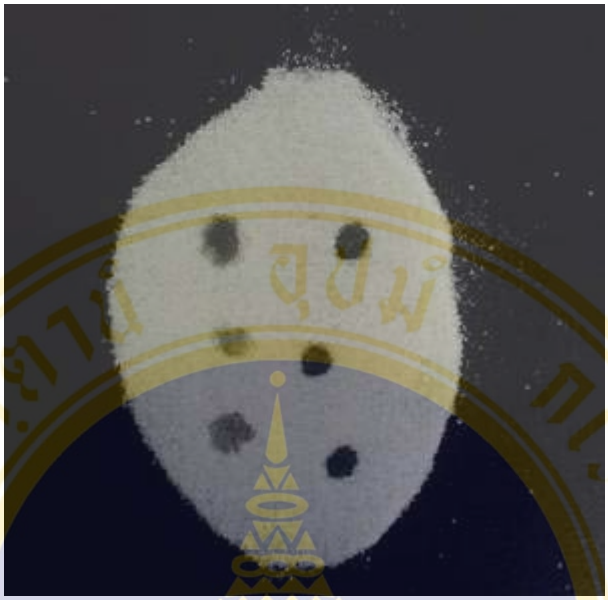

Figure 8 Gelatin which was dropped by water droplet

Figure 9 Pregelatinized starch which was dropped by water droplet

Figure 10 Cellulose fiber which was dropped by water droplet

Figure 11 Sample that consisted of 80% starch and 20% dextrin

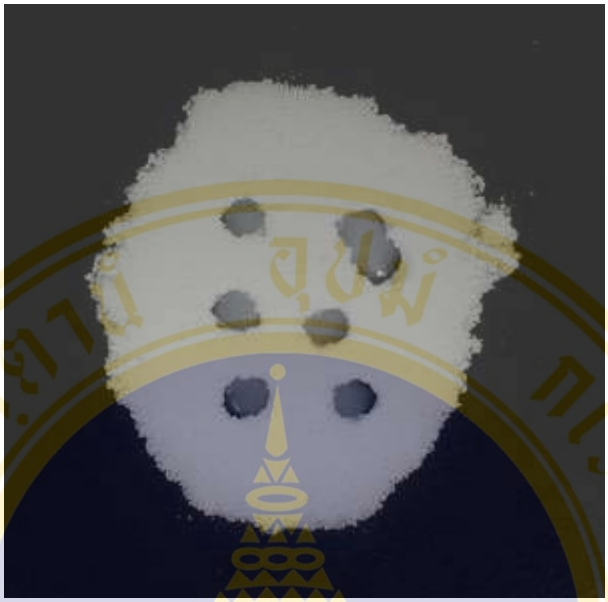

Figure 12 Sample that consisted of 20% starch and 80% dextrin

Figure 13 Sample that consisted of 50% starch and 50% dextrin

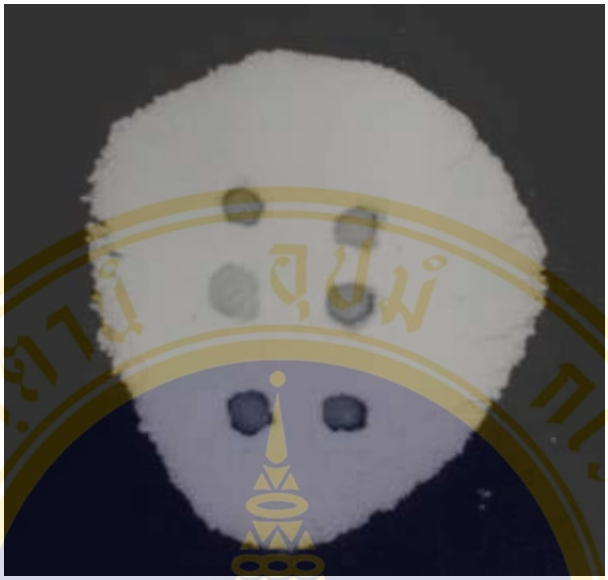

Figure 14 Sample that consisted of 40% starch, 40% dextrin and 20% pregelatinized starch

Figure 15 Sample that consisted of 40% starch, 40% dextrin and 20% cellulose fiber

Figure 16 Sample that consisted of 40% starch, 40% dextrin and 20% gelatin

Printing Parameters

The specimen of selected formulation, 40% starch, 40% dextrin and 20% gelatin was printed in 3DP machine with arrangement as shown in figure 17 by varying the conditions of printing such as layer thickness and saturation. The layer thickness was varied from 0.100 mm to 0.175 mm and saturation was varied from 100% to 70% as shown in Table 3. The results showed that the specimens were not able to be printed at layer thickness lower than 0.175 mm saturation greater than 70%. The lower in layer thickness or higher in saturation made the top layer to slip when it was spread by roller as shown in figure 18. Hence, all of the specimens in this experiment were printed with 70% saturation and 0.175 mm layer thickness.

Table 3 Printing characteristics

Saturation / Layer Thickness	100%	80%	70%
0.100 mm	slip	slip	slip
0.125 mm	slip	slip	slip
0.150 mm	slip	slip	slip
0.175 mm	slip	slip	not slip

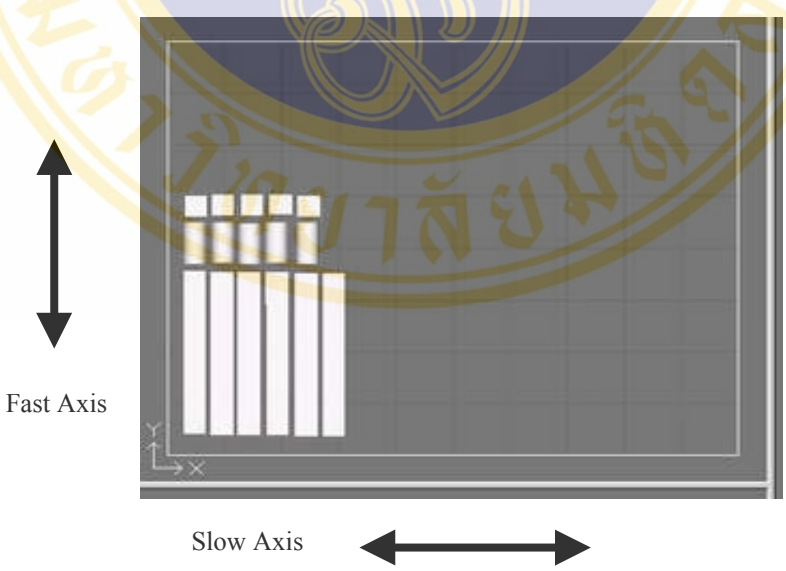

Figure 17 Specimens arrangement

Figure 18 Slipped layer

Dimensional Accuracy

The accuracy of the experimental samples and the original samples presented in Table 4 and 5 compared to the setting value. The results showed that the experimental sample has a higher percentage of error than the original sample in length and thickness dimensions but lower in width dimension. For both materials, the thickness has the greatest bleeding percentage while the length was the lowest.

Table 4 Dimensional error of samples

Samples	Dimensional Error (mm)		
	Width	Length	Thickness
S1	(+) 0.33_6 0.07	(+) 1.28_6 0.11	(+) 0.56_6 0.06
P	(+) 0.57_6 0.03	(+) 0.74_6 0.08	(+) 0.23_6 0.04

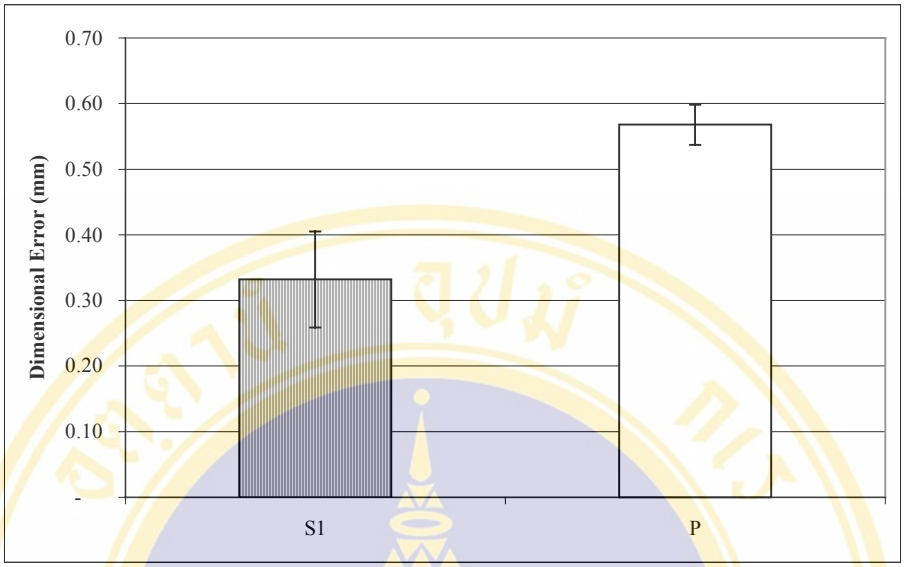

Figure 19 Width error of samples

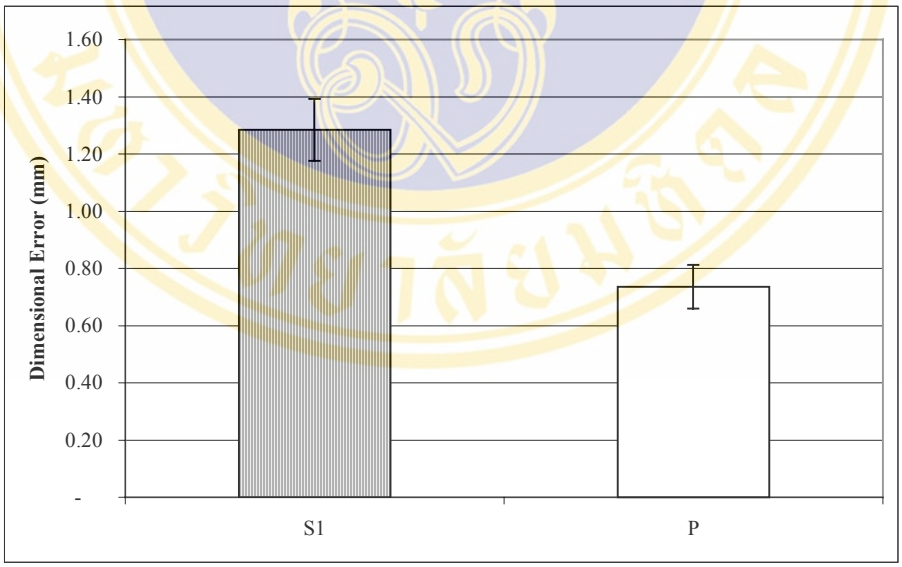

Figure 20 Length error of samples

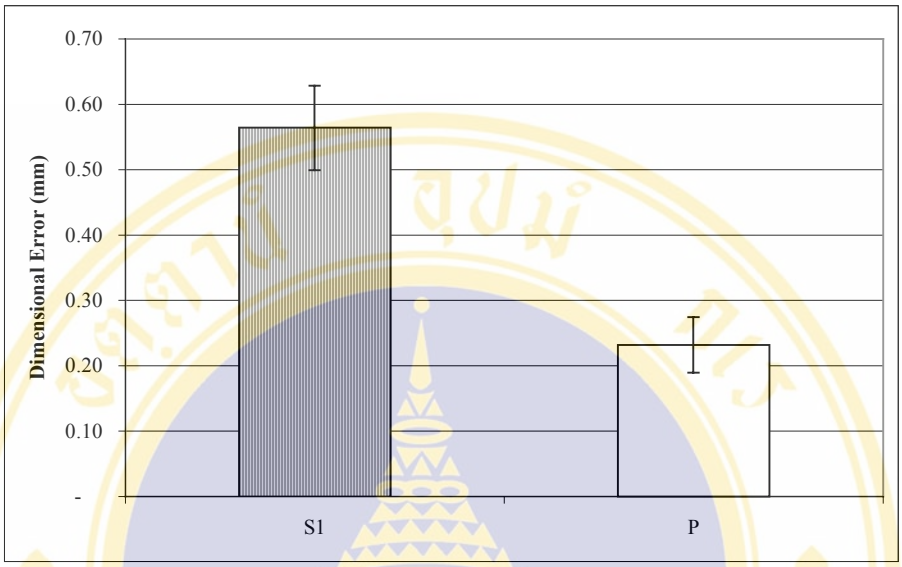

Figure 21 Thickness error of samples

Table 5 Percentage of dimensional error of samples

Samples	Error (%)		
	Width	Length	Thickness
S1	(+) 3.32 6 0.73	(+) 1.61 6 0.14	(+) 14.10 6 1.62
P	(+) 5.68 6 0.31	(+) 0.92 6 0.10	(+) 5.80 6 1.07

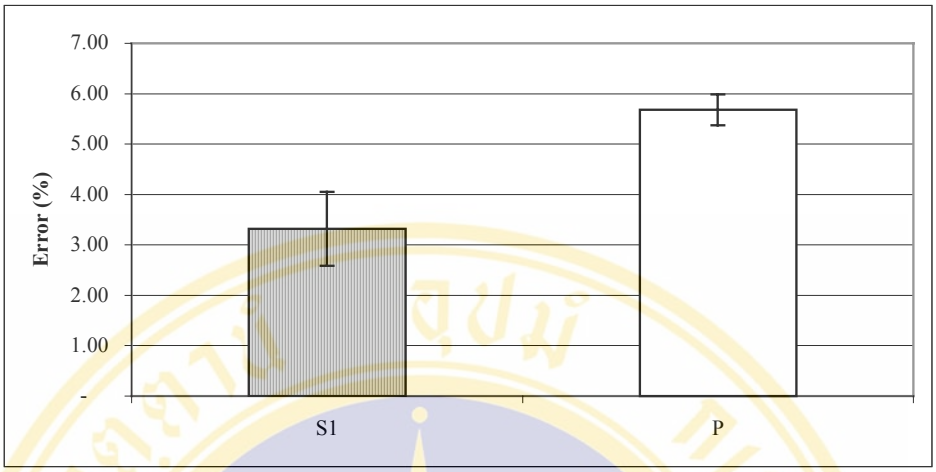

Figure 22 Percentage of width error of samples

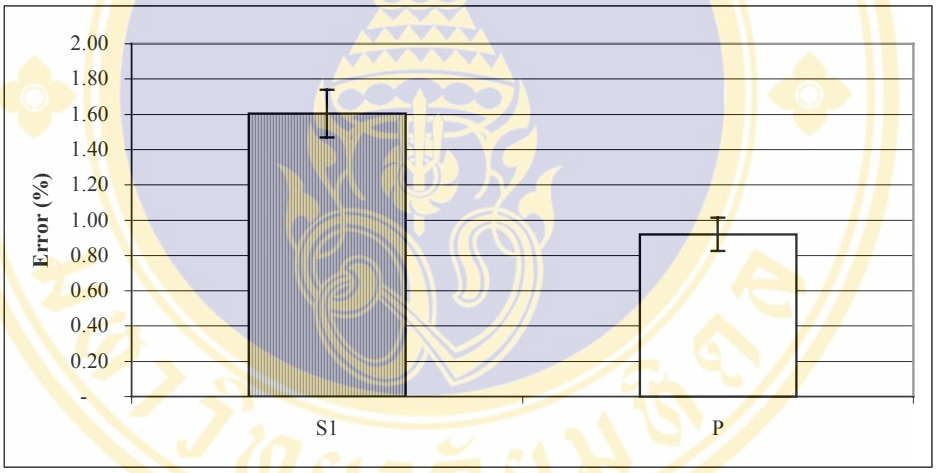

Figure 23 Percentage of length error of samples

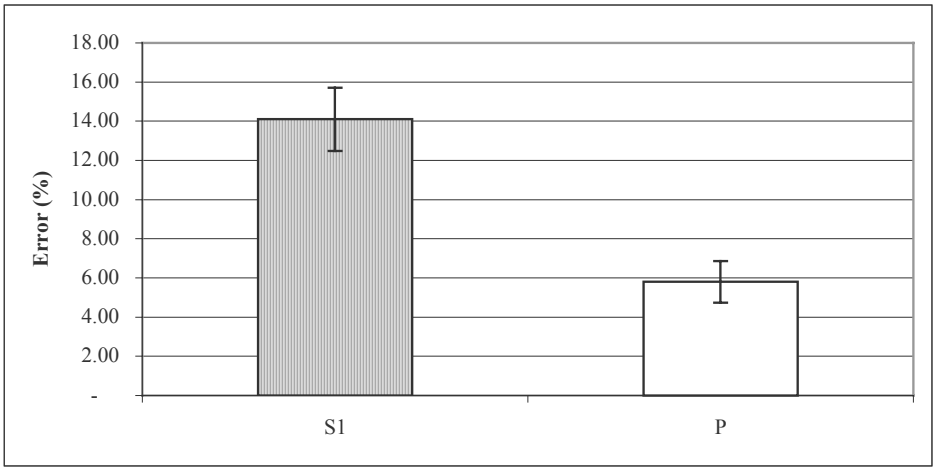

Figure 24 Percentage of thickness error of samples

Shrinkage

The average shrinkage of the experimental and the original samples are presented in Table 6. It can be observed that both experimental and original specimens tend to shrink after drying and the experimental specimen has a higher shrinkage.

Table 6 Shrinkage of samples

Samples	Shrinkage (%)		
	Width	Length	Thickness
S1	3.42 6 0.22	3.52 6 0.27	2.78 6 0.28
P	0.02 6 0.04	0.02 6 0.02	0.10 6 0.12

Density and Porosity

It can be seen that the experimental sample has a lower density but higher in porosity than the original sample for both dried and non-dried sample as presented in Table 7. Drying sample has a lower porosity than non-drying sample. In addition, there was a different set of samples for drying and non-drying type in each sample were used in this test.

Table 7 Density and porosity of samples

Samples	Apparent Density (g/cc)	True Density (g/cc)	Porosity (%)
S1-1	0.606 0.01	1.966 0.28	68.746 4.09
S1-2	0.566 0.01	1.616 0.04	65.076 1.43
P-1	0.956 0.01	2.686 0.41	63.906 5.18
P-2	0.986 0.01	2.336 0.06	57.736 1.19

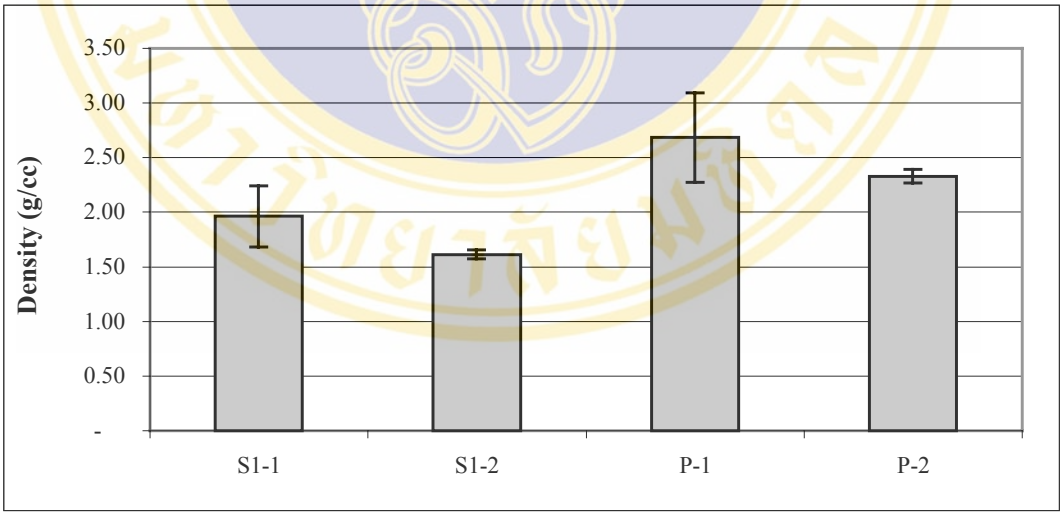

Figure 25 Apparent density of samples

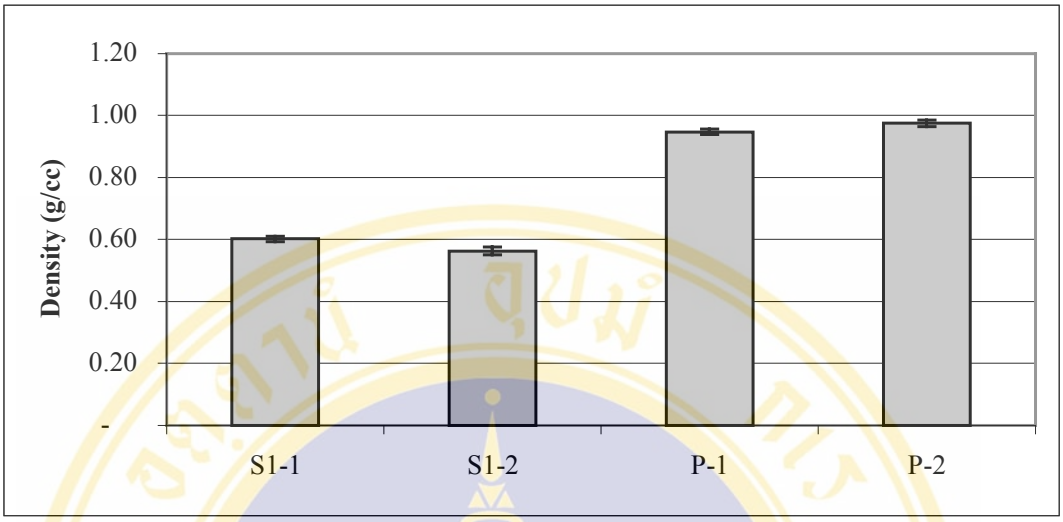

Figure 26 True density of samples

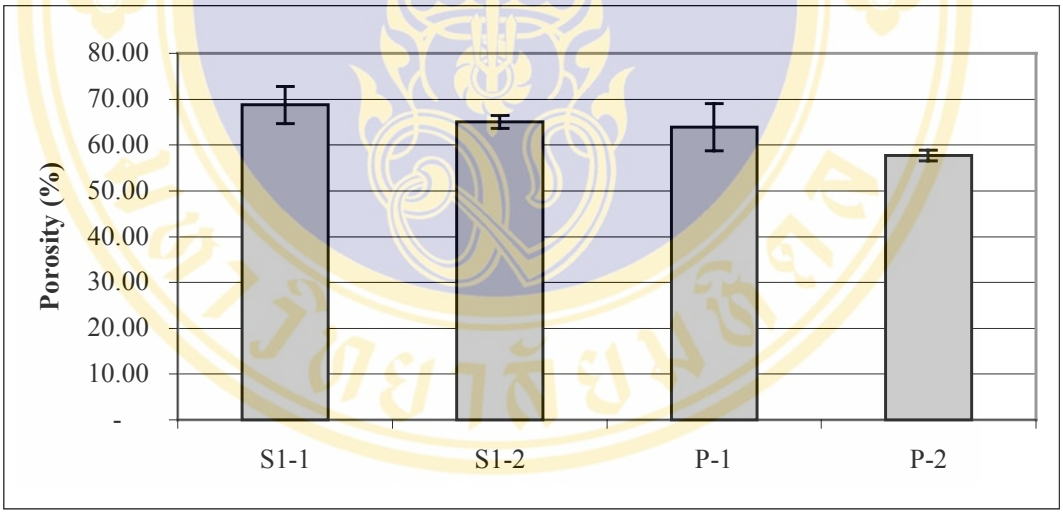

Figure 27 Porosity of samples

Mechanical Properties

The average bending and compressive strength are presented in Table 8. The mechanical strength of the original specimens is generally higher than the experimental specimens in both bending and compression. The drying samples

showed a greater strength than non-drying samples for both original and experimental samples significantly.

Table 8 Mechanical properties of samples

Samples	Strength (MPa)		Modulus (MPa)	
	Bending Strength	Compressive Strength	Bending	Compression
S1-1	0.97$_6$ 0.04	0.47$_6$ 0.10	246.96$_6$ 50.99	31.04$_6$ 6.50
S1-2	1.72$_6$ 0.50	0.61$_6$ 0.24	281.05$_6$ 89.65	40.32$_6$ 12.55
P-1	2.99$_6$ 0.12	4.02$_6$ 0.12	835.37$_6$ 58.03	148.86$_6$ 6.28
P-2	3.90$_6$ 0.10	4.61$_6$ 0.17	1037.06$_6$ 57.24	175.03$_6$ 9.72

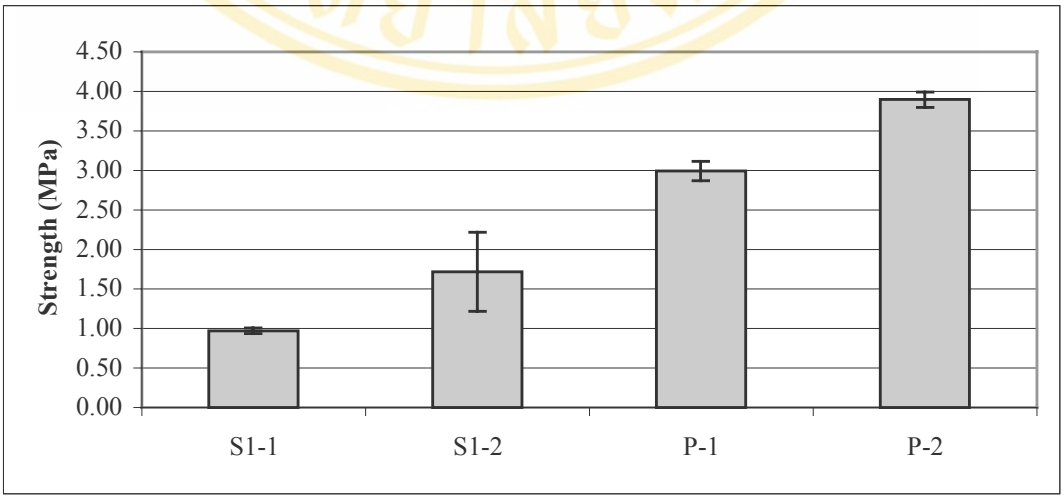

Figure 28 Bending strength of samples

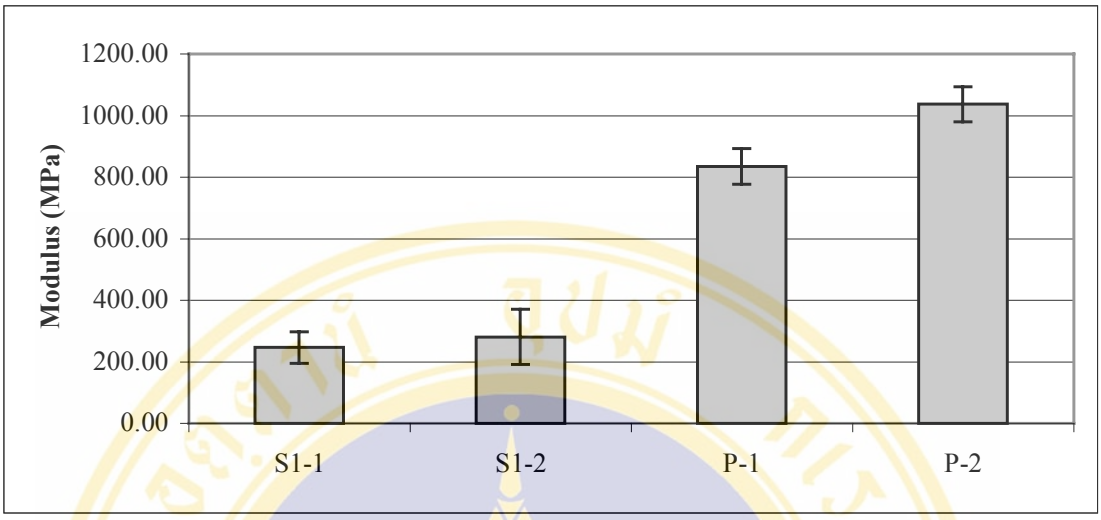

Figure 29 Bending modulus of samples

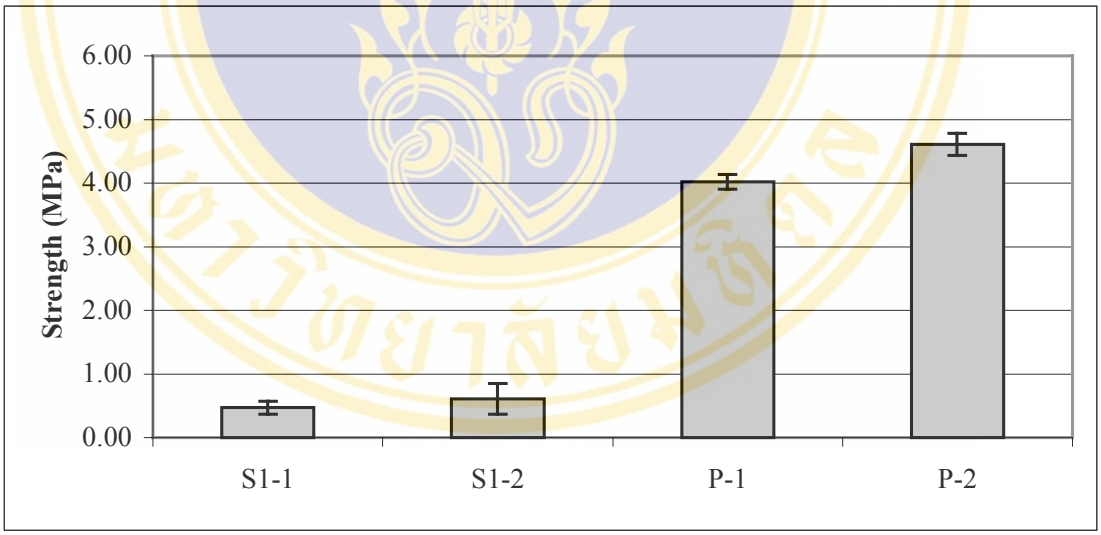

Figure 30 Compressive strength of samples

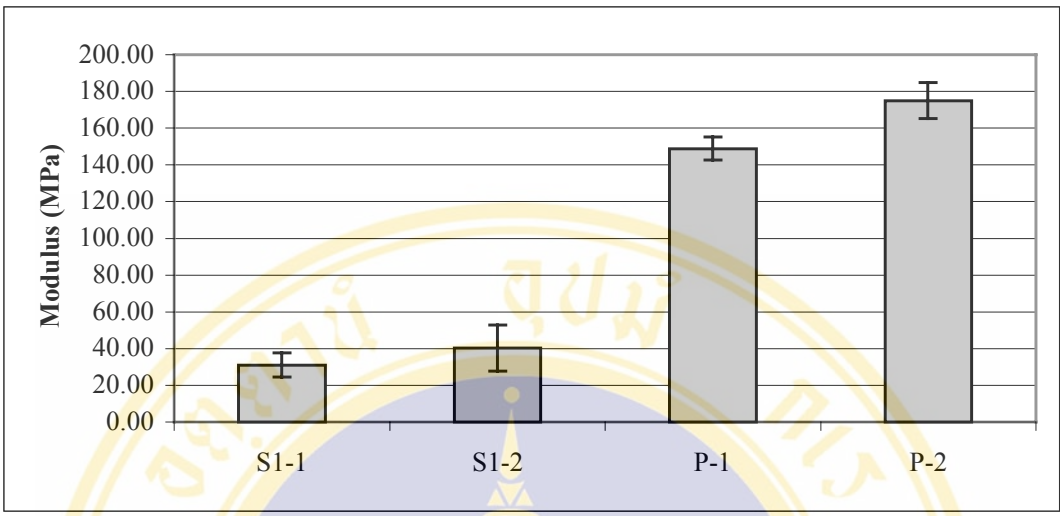

Figure 31 Compressive modulus of samples

CHAPTER V
DISCUSSION

1. Preliminary Observation

In preliminary observation, each material showed a different characteristics because of its difference in solubility and water holding capacity. Starch cannot be dissolved by water. When water droplet was dropped on the starch, it can spread easily through the starch particles. This resulted in the over spreading and without shrinkage, but has no strength. In contrast, dextrin that has higher solubility than the native starch and can be dissolved in cold water showed high shrinkage and good strength. Gelatin and pregelatinized starch were also insoluble in cold water, but turn to be gel after dispersion. Since the gel formation can trap the water in its molecule structure, the shrinkage and the over spreading problem did not occurre. However, the difference in mechanism of gel formation and structure between gelatin and pregelatinized starch made gelatin higher strength than pregelatinized starch. Cellulose fiber did not show the over spreading and shrinkage because it had a water holding capacity. However, its fiber matrix, which was swelled, might make the layer slip when it was printed by 3DP. Based on this result, gelatin was chosen to be an ingredient for the experimental powder (S1) in order to prevent the over spreading and shrinkage instead of pregelatinized starch and cellulose fiber [21].

2. Characteristics

The placement of part when printing affected directly to the object properties such as strength and accuracy. The object will be strongest and highest in accuracy along the y-axis and the x-axis and less strong in the z-axis because the layers are

printed in continuous steps along the y-axis, bands across the x-axis and laminated layers along the z-axis.

In this experiment, the thickness, which was printed along the z-axis was observed to have the highest in percentage of dimension error for both S1 and P sample as expected. However, the dimensional error can be fixed by bleed compensation adjustment in printing software.

The S1 material was not able to be printed at the saturation higher than 70% and less than 0.175 mm of layer thickness. The saturation that higher than 70% made the layer not dried sufficiently before the next layer was spread over by roller, this resulted in layers slippage. In comparison to the original printing that used 100% saturation and 0.1 mm layer thickness, the decrease in saturation and increase in layer thickness certainly will result in the decrease in strength and accuracy of the parts.

3. Characterization

The average particle sizes of the materials are in the range of 25-265 μm. It is slightly different from the average particle size of PLA (Polylactic acid), 75-150 μm, which has been printed by 3DP in the experiment of Giordano et al [12]. Therefore, the particle size of materials in this experiment should not affect to the printing ability.

Normally, material tends to shrink after drying because of the evaporation of moisture by heat. From the experiment, S1 sample exhibited high shrinkage (2.8-3.4%) after drying while, P sample which was made from plaster material exhibited lower (0.02-1.10%) than S1 sample. Because S1 sample which is made from starch and gelatin absorbed water by holding it in starch granules and gel matrix, whereas P sample used water in chemical reaction to solidified itself. Therefore, S1 sample that has more moisture left to evaporate than P1 sample presented higher shrinkage. However, it can be seen that the S1 sample has lower density but higher porosity than the P1 sample for both dried and non-dried sample. This is not surprising since plaster has higher density than natural polymers. The difference in porosity is thought to be caused by the difference in layer thickness and the saturation used between materials.

In addition, drying process that evaporated the moisture resulted in the decrease in porosity of samples.

Modulus and strength of the original sample is higher than the experimental sample in both bending and compression tests. This is caused by the difference in solidification mechanism between plaster based and natural polymers based materials. The crystallization of plaster, which is ceramic, when contacting with water will yield a stronger solid than the solidification of natural polymers by evaporation. Difference in layer thickness and saturation level also affected the mechanism properties. Higher saturation means that more binder is deposited so the degree of adherence is greater.

CHAPTER VI
CONCLUSIONS

The biomedical material that can be processed by 3DP technology was developed based on the blend of various natural polymers with different percentage and the results were concluded that.

1. The successful formula of the blended natural polymers for 3DP in this study consists of 40% starch, 40% dextrin and 20% gelatin.

2. The printing conditions that were appropriate to print the samples were 80% of saturation and 0.175 mm of layer thickness.

3. Experimental sample has higher shrinkage and porosity but less in density and mechanical properties.

Recommendations

Although, S1 mechanical properties are still less than P, there are several post-processing to increase it. The sample, which is a porous material, can be infiltrated by other strong biocompatible material is foreseen as a way to further improve the strength of this material. The infiltration not only increases the mechanical properties of sample but also decreases the water absorption, which is a required property for biomedical material. Other option is treating it with a vapor at high temperature. This will make the sample, which is made from starch, fully recrystalline.

REFERENCES

1. Wieneke-Toutaoui BM, Gerber HW. Rapid prototyping technology-new potentials for offshore and abyssal engineering [Online]. Berlin, Germany: TFH Berlin-University of Applied Sciences; 2003. Available from: http://www.tfh-berlin.de/~wieneke/ISOPE%202003-JSC-314.pdf [Accessed 2003 Nov 18].
2. Castle Island Co. Worldwide guide to rapid prototyping [Online]. Arlington (MA): 2003. Available from: http://home.att.net/~castleisland/rp_int.htm [Accessed 2003 Nov 19].
3. Department of mechanical engineering, Iowa state University. Rapid prototyping (RP) [Online]. Iowa: 2000. Available from: http://www.me.iastate.edu/me419_qamhiyah/course_modules/me419nrp.pdf [Accessed 2003 Nov 18].
4. Castle Island Co. Medical application of rapid prototyping [Online]. Arlington (MA): 2003. Available from: http://home.att.net/~castleisland/med_lks.htm [Accessed 2003 Nov 19].
5. Leong KF, Cheach CM, Chua CK. Solid freeform fabrication of three-dimensional scaffolds for engineering replacement tissues and organs. Biomaterials 2003;24:2363-78.
6. Chartoff R, Steidle C, Klosterman D, Graves G, Osborne N. Automated fabrication of custom bone implants using rapid prototyping [Online]. Long Beach (CA): 44th International SAMPE Symposium and Exhibition; 1999. Available from: http://www.udri.udayton.edu/rpdl/PDF_files/SAMPE99_bone.PDF [Accessed 2003 Nov 18].
7. Cook MN, Fisher JP, Dean D, Rimnac C, Mikos AG. Use of stereolithography to manufacture critical-sized 3D biodegradable scaffolds for bone ingrowth. J Biomed Mater Res 2003;64B(2):65-9.

8. Lee GH, Barlow JW. Selective laser sintering of calcium phosphate powders. Proceeding of the Solid Freeform Fabrication Symposium. Austin (TX): 1993. p. 191-7.

9. Tan KH, Chua CK, Leong KF, Cheah CM, Cheang P, Abu Bakar MS, Cha SW. Scaffold development using selective laser sintering of polyetheretherketone-hydroxyapatite biocomposite blends. Biomaterials 2003;24:3115-23.

10. Zein I, Hutmacher DW, Tan KC, Teoh SH. Fused deposition modeling of novel scaffold architectures for tissue engineering applications. Biomaterials 2002;23(4):1169-85.

11. Cornejo IA, Mcnulty TF, Lee S, Bianchi E, Danforth SC, Safari A. Development of bioceramic tissue scaffolds via fused deposition of ceramics. In: George L, editor. Bioceramics: materials and application III. Westerville (OH): American Ceramic Society; 2000. p. 183-95

12. Giordano RA, Wu BM, Borland SW, Cima LG, Sachs EM, Cima MJ. Mechanical properties of dense polylactic acid structures fabricated by three dimensional printing. J Biomater Sci Polym Ed 1996;8(1):63-75.

13. Lam CXF, Mo XM, Teoh SH, Hutmacher DW. Scaffold development using 3D printing with a starch-based polymer. Mater Sci Eng C 2002;20(1-2): 49-56.

14. Mendes SC, Reis RL, Bovell YP, Cunha AM, van Blitterswijk CA, de Bruijin JD. Biocompatibility testing of novel starch-based materials with potential application in orthopaedic surgery: a preliminary study. Biomaterials 2001;22:2057-64.

15. Marques AP, Reis RL, Hunt JA. The biocompatibility of novel starch-based polymers and composites: in vitro studies. Biomaterials 2002;23:1471-8.

16. Lopes CMA, Felisberti MI. Mechanical behaviour and biocompatibility of poly (1-vinyl-2-pyrrolidinone)-gelatin IPN hydrogels. Biomaterials 2003;24:1279-84.

17. Zhou F, Vervaet C, Schelkens M, Lefebvre R, Remon JP. Bioavailability of ibuprofen from matrix pellets based on the combination of waxes and starch derivatives. International Journal of Pharmaceutics 1998;168: 79-84.
18. Te Wierik GHP, Eissens AC, Bergsma J, Arends-Scholte AW, Bolhuis GK. A new generation starch product as excipient in pharmaceutical tablets. International Journal of Pharmaceutics 1997;157:181-7.
19. Katz DL, Nawaz H, Boukhalil J, Chan W, Ahamadi R, Giannamore V, et al. Effect of oat and wheat cereals on endothelial responses. Preventive Medicine 2001;33:476-84.
20. Robert SI, Yiu HH. Dictionary of food ingredients. 4 th ed. Maryland: Aspen; 2001.
21. Macrae R, Robinson RK, Sadler MJ. Encycopedia of food science, food technology, and nutrition. San Diego: Academic Press Inc; 1993.

APPENDIX

APPENDIX

Appendix 1 Results of particle size determination

Sample Type	Sample No.	Volume Distribution			Mean Diameters
		10%	50%	90%	
starch	1	9.30	19.88	45.23	25.19
	2	9.25	20.19	49.18	26.41
	3	9.07	19.40	43.77	24.50
	Average	9.21	19.82	46.06	**25.37**
	SD	0.09	0.28	1.98	**0.79**
dextrin	1	32.94	83.49	160.74	90.76
	2	32.71	82.95	159.72	90.20
	3	32.55	82.81	159.72	90.10
	Average	32.73	83.08	160.06	**90.35**
	SD	0.14	0.25	0.42	**0.29**
gelatin	1	80.65	227.97	512.82	266.12
	2	77.14	221.68	508.98	261.32
	3	80.65	229.08	515.68	267.37
	Average	79.48	226.24	512.49	**264.94**
	SD	1.43	2.82	2.38	**2.61**
pre-starch	1	30.53	87.94	177.55	96.95
	2	30.52	88.13	178.14	97.20
	3	30.60	88.51	179.36	97.72
	Average	30.55	88.19	178.35	**97.29**
	SD	0.03	0.21	0.65	**0.32**
fiber	1	18.04	103.11	255.12	122.32
	2	17.78	104.14	260.00	124.60
	3	17.58	103.90	259.79	124.41
	Average	17.80	103.72	258.30	**123.78**
	SD	0.16	0.38	1.95	**1.03**

Appendix 2 Results of dimensional error

Sample Type	Sample No.	Dimensional error (mm)			Percentage error (%)		
		width	length	thickness	width	length	thickness
S1	1	0.36	1.16	0.62	3.60	1.45	15.50
	2	0.39	1.17	0.48	3.90	1.46	12.00
	3	0.21	1.45	0.49	2.10	1.81	12.25
	4	0.41	1.33	0.61	4.10	1.66	15.25
	5	0.29	1.31	0.62	2.90	1.64	15.50
	Average	**0.33**	**1.28**	**0.56**	**3.32**	**1.61**	**14.10**
	SD	**0.07**	**0.11**	**0.06**	**0.73**	**0.14**	**1.62**
P	1	0.61	0.68	0.28	6.10	0.85	7.00
	2	0.52	0.86	0.23	5.20	1.08	5.75
	3	0.58	0.64	0.28	5.80	0.80	7.00
	4	0.55	0.73	0.19	5.50	0.91	4.75
	5	0.58	0.77	0.18	5.80	0.96	4.50
	Average	**0.57**	**0.74**	**0.23**	**5.68**	**0.92**	**5.80**
	SD	**0.03**	**0.08**	**0.04**	**0.31**	**0.10**	**1.07**

Appendix 3 Results of shrinkage determination

Sample Type	Sample No.	Dimensions before drying (mm)			Dimensions after drying (mm)			Shrinkage (%)		
		width	length	thickness	width	length	thickness	width	length	thickness
S1	1	10.33	81.49	4.56	9.99	78.84	4.41	3.29	3.25	3.29
	2	10.39	81.20	4.53	10.03	78.65	4.40	3.46	3.14	2.87
	3	10.33	81.53	4.48	9.97	78.48	4.36	3.48	3.74	2.68
	4	10.30	81.49	4.45	9.98	78.38	4.34	3.11	3.82	2.47
	5	10.39	81.44	4.62	10.00	78.47	4.50	3.75	3.65	2.60
	Average	**10.35**	**81.43**	**4.53**	**9.99**	**78.56**	**4.40**	**3.42**	**3.52**	**2.78**
	SD	**0.04**	**0.12**	**0.06**	**0.02**	**0.16**	**0.06**	**0.22**	**0.27**	**0.28**
P	1	10.01	80.53	4.07	10.01	80.50	4.06	0.00	0.04	0.25
	2	10.03	80.61	4.09	10.03	80.60	4.09	0.00	0.01	0.00
	3	9.91	80.52	4.02	9.90	80.51	4.02	0.10	0.01	0.00
	4	10.01	80.48	4.03	10.01	80.48	4.02	0.00	0.00	0.25
	5	10.03	80.58	4.02	10.03	80.53	4.02	0.00	0.06	0.00
	Average	**8.00**	**64.45**	**3.25**	**7.99**	**64.45**	**3.25**	**0.02**	**0.02**	**0.10**
	SD	**0.04**	**0.05**	**0.03**	**0.05**	**0.04**	**0.03**	**0.04**	**0.02**	**0.12**

Appendix 4 Results of density and porosity determination

Sample Type	Sample No.	Weight (g)	Width (mm)	Length (mm)	Thickness (mm)	Apparent		True		Porosity (%)
						Volume (cc)	Density (g/cc)	Volume (cc)	Density (g/cc)	
S1-1	1	0.27	10.15	10.40	4.38	0.46	0.59	0.17	1.63	63.66
	2	0.29	10.03	10.50	4.65	0.49	0.59	0.17	1.68	64.73
	3	0.27	10.18	10.22	4.34	0.45	0.60	0.12	2.33	74.13
	4	0.29	10.09	10.52	4.56	0.48	0.61	0.15	1.96	68.87
	5	0.30	10.08	10.64	4.50	0.48	0.61	0.13	2.21	72.30
	Average	**0.29**	**10.11**	**10.46**	**4.49**	**0.47**	**0.60**	**0.15**	**1.96**	**68.74**
	SD	**0.01**	**0.05**	**0.14**	**0.11**	**0.01**	**0.01**	**0.02**	**0.28**	**4.09**
S1-2	1	0.27	10.18	10.44	4.44	0.47	0.57	0.17	1.56	63.53
	2	0.26	10.18	10.38	4.50	0.48	0.54	0.15	1.67	67.61
	3	0.25	10.20	10.19	4.35	0.45	0.56	0.16	1.57	64.44
	4	0.26	10.14	10.35	4.44	0.47	0.57	0.16	1.65	65.58
	5	0.26	10.05	10.37	4.34	0.45	0.58	0.16	1.62	64.21
	Average	**0.26**	**10.15**	**10.35**	**4.41**	**0.46**	**0.56**	**0.16**	**1.61**	**65.07**
	SD	**0.01**	**0.05**	**0.08**	**0.06**	**0.01**	**0.01**	**0.01**	**0.04**	**1.43**
P-1	1	0.39	9.82	10.38	4.10	0.42	0.93	0.16	2.39	60.97
	2	0.40	9.89	10.47	4.11	0.43	0.94	0.13	3.15	70.04
	3	0.40	9.87	10.34	4.06	0.41	0.96	0.12	3.22	70.31
	4	0.39	9.86	10.35	4.07	0.42	0.94	0.17	2.32	59.24
	5	0.41	9.78	10.50	4.12	0.42	0.96	0.17	2.34	58.92
	Average	**0.40**	**9.84**	**10.41**	**4.09**	**0.42**	**0.95**	**0.15**	**2.68**	**63.90**
	SD	**0.01**	**0.04**	**0.06**	**0.02**	**0.00**	**0.01**	**0.02**	**0.41**	**5.18**
P-2	1	0.41	9.83	10.38	4.12	0.42	0.98	0.17	2.38	58.63
	2	0.39	9.85	10.28	4.02	0.41	0.96	0.17	2.25	57.48
	3	0.40	9.90	10.31	4.01	0.41	0.97	0.17	2.39	59.49
	4	0.41	9.96	10.31	4.02	0.41	0.99	0.18	2.26	56.25
	5	0.40	9.86	10.30	4.01	0.41	0.98	0.18	2.26	56.78
	Average	**0.40**	**9.88**	**10.32**	**4.04**	**0.41**	**0.98**	**0.17**	**2.31**	**57.73**
	SD	**0.01**	**0.05**	**0.03**	**0.04**	**0.00**	**0.01**	**0.00**	**0.06**	**1.19**

Appendix 5 Results of bending test

Sample Type	Sample No.	Width (mm)	Length (mm)	Thickness (mm)	Bending	
					Strength (MPa)	Modulus (MPa)
S1-1	1	10.36	81.16	4.62	0.93	253.30
	2	10.39	81.17	4.48	1.02	259.72
	3	10.21	81.45	4.49	0.95	204.14
	4	10.41	81.33	4.61	0.94	331.91
	5	10.29	81.31	4.62	1.01	185.76
	Average	**10.33**	**81.28**	**4.56**	**0.97**	**246.96**
	SD	**0.07**	**0.11**	**0.06**	**0.04**	**50.99**
S1-2	1	9.99	78.84	4.41	1.18	171.50
	2	10.03	78.65	4.40	1.20	175.99
	3	9.97	78.48	4.36	2.27	349.11
	4	9.98	78.38	4.34	2.33	384.12
	5	10.00	78.47	4.50	1.62	324.52
	Average	**9.99**	**78.56**	**4.40**	**1.72**	**281.05**
	SD	**0.02**	**0.16**	**0.06**	**0.50**	**89.65**
P-1	1	10.00	80.52	4.11	2.90	875.26
	2	10.00	80.50	4.12	2.93	890.85
	3	10.01	80.76	4.10	3.13	822.53
	4	10.05	80.71	4.15	3.15	859.68
	5	10.08	80.46	4.12	2.86	728.53
	Average	**10.03**	**80.59**	**4.12**	**2.99**	**835.37**
	SD	**0.03**	**0.12**	**0.02**	**0.12**	**58.03**
P-2	1	10.36	81.16	4.62	3.82	983.61
	2	10.39	81.17	4.48	3.95	970.44
	3	10.21	81.45	4.49	3.94	1063.14
	4	10.41	81.33	4.61	4.02	1128.71
	5	10.29	81.31	4.62	3.75	1039.42
	Average	**10.33**	**81.28**	**4.56**	**3.90**	**1037.06**
	SD	**0.05**	**0.04**	**0.03**	**0.10**	**57.24**

Appendix 6 Results of compressive testing

Sample Type	Sample No.	Diameter (mm)	Height (mm)	Compressive	
				Strength (MPa)	Modulus (MPa)
S1-1	1	10.16	20.79	0.39	32.71
	2	10.01	20.55	0.38	21.41
	3	10.02	20.59	0.41	25.94
	4	10.04	20.77	0.56	36.10
	5	10.06	20.59	0.63	39.06
	Average	**10.06**	**20.66**	**0.47**	**31.04**
	SD	**0.05**	**0.10**	**0.10**	**6.50**
S1-2	1	9.81	20.32	0.34	24.38
	2	9.95	20.30	0.29	30.99
	3	9.57	19.87	0.75	36.48
	4	9.63	19.97	0.82	52.78
	5	9.71	20.12	0.84	56.95
	Average	**9.73**	**20.12**	**0.61**	**40.31**
	SD	**0.13**	**0.18**	**0.24**	**12.55**
P-1	1	10.01	20.24	3.85	146.85
	2	9.94	20.32	4.02	152.72
	3	10.07	20.46	3.94	137.43
	4	10.06	20.38	4.12	154.65
	5	9.96	20.36	4.17	152.65
	Average	**10.01**	**20.35**	**4.02**	**148.86**
	SD	**0.05**	**0.07**	**0.12**	**6.28**
P-2	1	10.09	20.53	4.58	169.25
	2	10.17	20.43	4.47	168.62
	3	9.93	20.58	4.90	193.45
	4	9.97	20.47	4.66	176.34
	5	10.08	20.27	4.42	167.47
	Average	**10.05**	**20.46**	**4.61**	**175.03**
	SD	**0.09**	**0.11**	**0.17**	**9.72**

BIOGRAPHY

NAME	Mr. Passakorn Tesavibul
DATE OF BIRTH	23 December, 1976
PLACE OF BIRTH	Bangkok, Thailand
INSTITUTIONS ATTENDED	Srinakarinwirot University, 1994-1998 Bachelor of Engineering (Industrial Engineering) Mahidol University, 2001-2004 Master of Engineering (Biomedical Engineering)
HOME ADDRESS	424/708 Rajvithi road, Rajtavee, Bangkok Tel. 0-2202-5213